ALLERGY

Clonally expanded, GPR15-expressing pathogenic effector T_H2 cells are associated with eosinophilic esophagitis

Duncan M. Morgan[1,2], Bert Ruiter[3,4], Neal P. Smith[3], Ang A. Tu[1,5,6], Brinda Monian[1,2], Brandon E. Stone[3], Navneet Virk-Hundal[7], Qian Yuan[7], Wayne G. Shreffler[3,4,7]*, J. Christopher Love[1,2,8,9]*

Eosinophilic esophagitis (EoE) is an allergic disorder characterized by the recruitment of eosinophils to the esophagus, resulting in chronic inflammation. We sought to understand the cellular populations present in tissue biopsies of patients with EoE and to determine how these populations are altered between active disease and remission. To this end, we analyzed cells obtained from esophageal biopsies, duodenal biopsies, and peripheral blood of patients with EoE diagnosed with active disease or remission with single-cell RNA and T cell receptor (TCR) sequencing. Pathogenic effector T_H2 (peT_H2) cells present in the esophageal biopsies of patients with active disease expressed distinct gene signatures associated with the synthesis of eicosanoids. The esophageal tissue–resident peT_H2 population also exhibited clonal expansion, suggesting antigen-specific activation. Peripheral $CRTH2^+CD161^-$ and $CRTH2^+CD161^+$ memory $CD4^+$ T cells were enriched for either a conventional T_H2 phenotype or a peT_H2 phenotype, respectively. These cells also exhibited substantial clonal expansion and convergence of TCR sequences, suggesting that they are expanded in response to a defined set of antigens. The esophagus-homing receptor *GPR15* was up-regulated by peripheral peT_H2 clonotypes that were also detected in the esophagus. Finally, $GPR15^+$ peT_H2 cells were enriched among milk-reactive $CD4^+$ T cells in patients with milk-triggered disease, suggesting that these cells are an expanded, food antigen–specific population with enhanced esophagus homing potential.

INTRODUCTION

Eosinophilic esophagitis (EoE) is an allergic disease characterized by chronic esophageal inflammation with prominent recruitment of eosinophils, resulting in difficulty swallowing, food impaction, and esophageal dysfunction (*1*, *2*). Clinically, EoE often manifests as an antigen-specific disease, in which exposure to specific food-derived allergens triggers esophageal inflammation (*3*), but evidence for an antigen-specific adaptive immune response in EoE is lacking. Inflammation in EoE involves T helper 2 (T_H2) cells that produce the cytokines interleukin-5 (IL-5), which promotes eosinophil recruitment and activation, and IL-13, which exacerbates epithelial barrier dysfunction (*2*, *4*, *5*). Much of the available transcriptional and genetic data, however, appear to place dysregulation of an epithelial unit at the center of disease pathogenesis (*5*–*7*). In addition, although patients with EoE exhibit increased numbers of highly polarized pathogenic effector T_H2 (peT_H2) cells in the periphery, these cells have "innate-like" phenotypic characteristics, such as the expression of receptors for IL-25 and IL-33, that may allow sustained inflammation in the absence of specific antigen stimulation (*8*, *9*).

Recent single-cell RNA sequencing studies have confirmed that such peT_H2 cells reside in the esophageal tissue of patients with EoE, but the limited numbers of these cells recovered precluded comprehensive assessment of the clonal relationships within this population (*9*). Ultimately, the signaling pathways that lead to the recruitment of peT_H2 cells to the esophagus and the full set of mechanisms through which these cells mediate eosinophil recruitment and chronic esophageal inflammation remain unknown. Furthermore, the clonal identities and antigen specificities of these cells have yet to be determined.

To better understand the cellular mechanisms underlying EoE, we conducted a single-cell genomic analysis of the types and functions of cells present in esophageal biopsies, duodenal biopsies, and peripheral blood of patients with EoE. We identified a population of T cells that expressed peT_H2 markers and was enriched in the esophageal biopsies of patients with active disease. This population up-regulated expression of T_H2 cytokines and genes related to lipid metabolism and also exhibited clonal expansion, consistent with antigen-dependent activation. In peripheral blood of the same patients, we detected clonotypes with a peT_H2 phenotype that were shared with those detected in tissue. Peripheral peT_H2 clonotypes that were also detected in the esophagus up-regulated the gene for the esophagus-homing receptor *GPR15*. These results suggest that $GPR15^+$ peT_H2 cells in EoE are an antigen-specific population with enhanced esophagus homing potential.

RESULTS

Mapping the single-cell ecosystem of EoE

We first analyzed cells dissociated from tissue biopsies collected from 10 patients with EoE. Six of these patients were diagnosed with active disease at the time of biopsy, and four patients were diagnosed with disease in remission (table S1). From each patient, we collected up to six biopsies from the esophagus and duodenum. The cells recovered from these biopsies were processed for single-cell RNA sequencing with Seq-Well (Fig. 1A) (*10*, *11*). From these tissue biopsies, we recovered a total of 28,816 high-quality single-cell transcriptomes with greater than 500 unique genes detected (fig. S1).

[1]Koch Institute for Integrative Cancer Research, MIT, Cambridge, MA, USA. [2]Department of Chemical Engineering, MIT, Cambridge, MA, USA. [3]Center for Immunology and Inflammatory Diseases, Massachusetts General Hospital, Boston, MA, USA. [4]Harvard Medical School, Boston, MA, USA. [5]Department of Biological Engineering, MIT, Cambridge, MA, USA. [6]Immunitas Therapeutics Inc., Cambridge, MA, USA. [7]Food Allergy Center, Massachusetts General Hospital, Boston, MA, USA. [8]Broad Institute of MIT and Harvard, Cambridge, MA, USA. [9]Ragon Institute of MGH, MIT and Harvard, Cambridge, MA, USA.
*Corresponding author. Email: wshreffler@mgh.harvard.edu (W.G.S.); clove@mit.edu (J.C.L.)

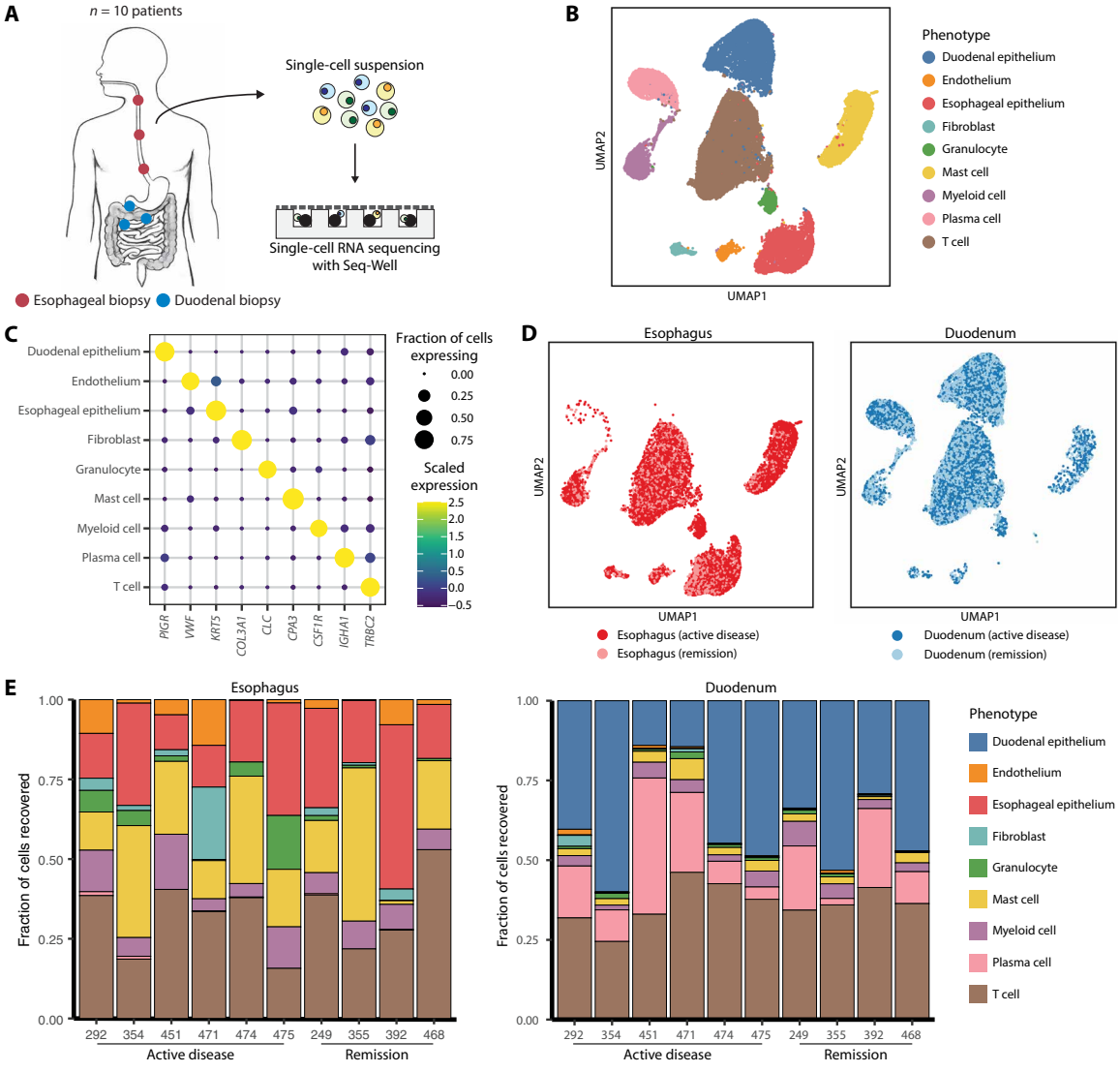

Fig. 1. Single-cell RNA sequencing of esophageal and duodenal biopsies of patients with EoE. (**A**) Schematic of biopsy processing pipeline. Biopsies from 10 patients with EoE (6 with active disease and 4 in remission) were enzymatically dissociated into single-cell suspensions and processed for single-cell RNA sequencing using Seq-Well. (**B**) UMAP of 28,816 cells obtained from the esophageal and duodenal biopsies of 10 patients with EoE, colored by cell phenotype. (**C**) Dot plots of select marker genes for each cell phenotype displaying average expression and frequency of expression for each gene. (**D**) UMAP of cells obtained from esophageal and duodenal biopsies colored by tissue and patient diagnosis. (**E**) Bar plots depicting relative frequencies of cell phenotypes from the esophageal and duodenal biopsies of each patient.

The resulting gene expression matrix was processed using dimensionality reduction and was visualized with uniform manifold approximation and projection (UMAP) (*12*). Using graph-based clustering, we identified nine major clusters corresponding to different cell types (Fig. 1B). These clusters were annotated according to the expression of marker genes and corresponded to T cells, plasma cells, granulocytes, mast cells, myeloid cells, fibroblasts, endothelial cells, esophageal epithelial cells, and duodenal epithelial cells (Fig. 1C, figs. S2 and S3, and data file S1). The frequency of some cell populations varied largely between the esophagus and the duodenum; minor variation in the frequencies of these clusters in each tissue between patients may result from patient-intrinsic differences, such as age, and technical factors, such as variations in cell viability or the tissue dissociation process (Fig. 1, D and E). Epithelial cells were less frequent than expected in biopsies from both the esophagus and duodenum, suggesting that the larger sizes of these cells may bias against their entry into the wells on the Seq-Well arrays, resulting in an enrichment for populations with smaller size. Despite this technical factor, classical marker genes of EoE, including epithelial-associated transcripts such as *CCL26*, *POSTN*, and *CAPN14* were up-regulated in esophageal biopsies from patients with active disease, supporting that the single-cell sequencing data had high fidelity (fig. S4).

Eosinophils in the esophagus during active disease activate pathways regulated by nuclear factor κB

The presence of eosinophils in the esophagus is the primary criterion for the diagnosis for EoE (*1*, *2*, *4*). At higher resolution, the cluster

of granulocytes not only was composed primarily of eosinophils but also contained a small population of neutrophils (Fig. 2, A and B). The eosinophils expressed genes for the surface markers *SIGLEC8*, *CCR3*, *PTGDR2*, and *IL5RA* as well as genes that encode for granule components, such as *CLC* (galectin-10) and *RNASE2* (eosinophil-derived neurotoxin) (Fig. 2C). In contrast, the neutrophils expressed high levels of the genes for the surface markers *CXCR2*, *FCGR3A*, and *FCGR3B* (Fig. 2C). Other granule-associated proteins, including *PRG2* (major basic protein), *EPX* (eosinophil peroxidase), and *RNASE3* (eosinophil cationic protein) were not strongly expressed in eosinophils, consistent with prior reports that these proteins are primarily synthesized during eosinophil maturation and that the transcripts are not expressed in mature eosinophils (*13*, *14*).

The fraction of eosinophils in the esophagus, calculated as the fraction of total recovered single cells, was significantly increased in patients with active disease, although one patient in remission had a slightly elevated frequency of eosinophils (Fig. 2D). An average of 4.7% of single cells recovered from the esophageal biopsies of patients with active disease were eosinophils. Eosinophils were also detected in the duodenal biopsies of all 10 patients, but their frequency did not significantly differ between active disease and remission (Fig. 2D). We observed a correlation between the number of eosinophils determined

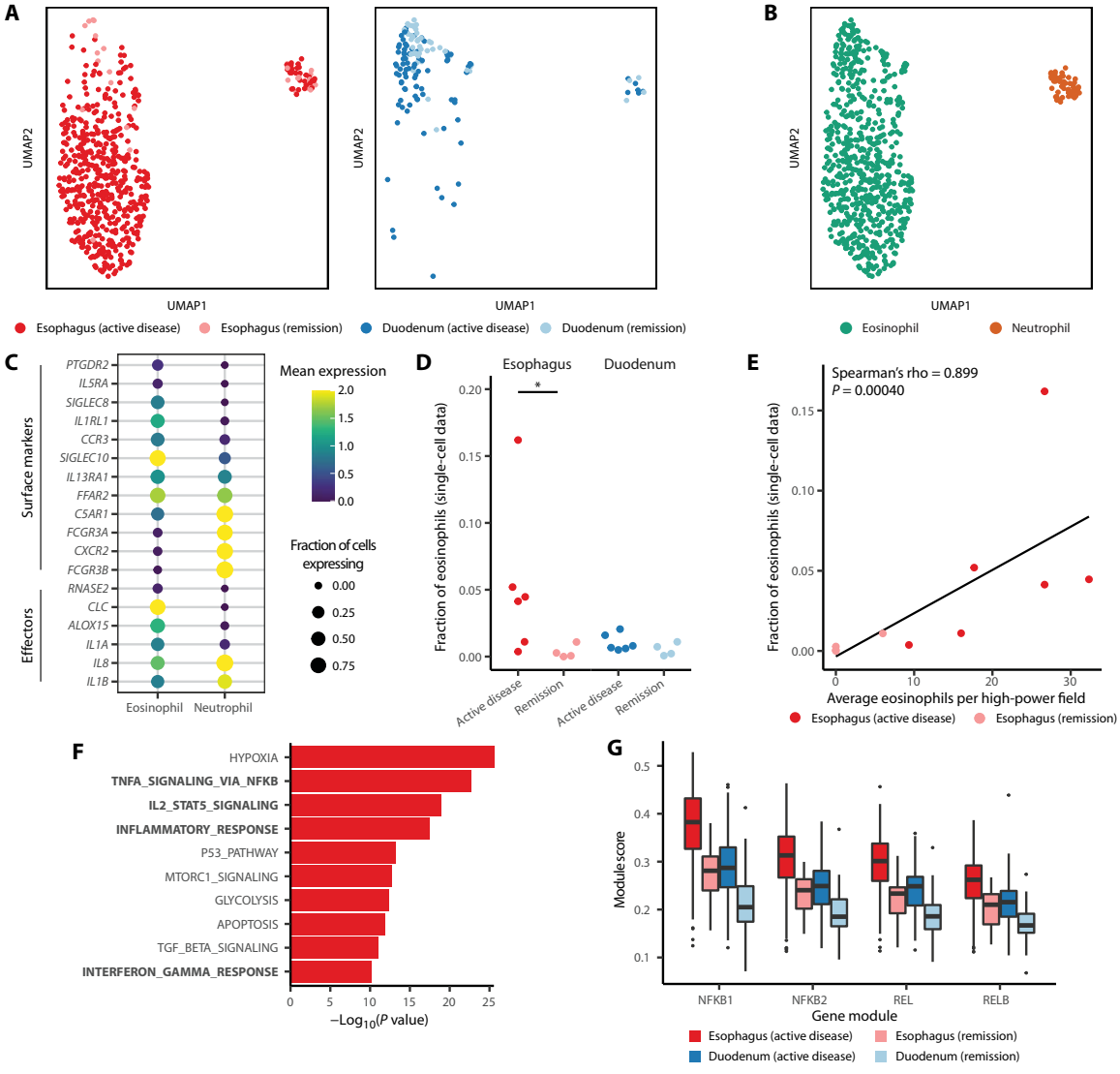

Fig. 2. Eosinophils are enriched and activated in the esophagus during active disease. (**A**) UMAP of granulocyte cluster colored by tissue and disease status ($n = 679$ cells). (**B**) UMAP of granulocyte cluster colored by type of granulocyte. (**C**) Dot plots of select surface markers and inflammatory effectors expressed by eosinophils and neutrophils displaying average expression and frequency of expression for each gene. (**D**) Fraction of cells in single-cell data that were classified as eosinophils from esophageal or duodenal biopsies of patients in disease or remission. *P* values were computed using a two-sided Wilcoxon rank sum test (*$P < 0.05$). (**E**) Correlation between number of eosinophils per high-power field in esophageal tissue determined with histological staining and fraction of eosinophils recovered from esophageal biopsies with single-cell RNA sequencing. Spearman's correlation coefficient and the associated *P* value are shown. (**F**) Pathways up-regulated in eosinophils present in the esophageal tissue of patients with active disease relative to eosinophils in the duodenum. *P* values are calculated with a two-sided Wilcoxon rank sum test and are adjusted with Bonferroni correction. (**G**) Transcription factor module scores produced by SCENIC for modules regulated by subunits of NF-κB.

by histological staining and the fraction of eosinophils in our single-cell dataset, indicating concordance between the observations with single-cell RNA sequencing and with those from tissue staining (Fig. 2E).

To determine how eosinophils respond to inflammatory signals produced in EoE, we identified pathways that were up-regulated by eosinophils in the esophagus during active disease relative to eosinophils in the duodenum, where inflammation is not typically histologically evident (*15*). We found that several proinflammatory pathways, including "IL-2/STAT5 signaling," "TNF signaling via NF-κB," and "inflammatory response" were up-regulated by esophageal eosinophils during active disease (Fig. 2F), indicating that eosinophils recruited to the esophagus in EoE are activated during active disease. To elucidate gene regulatory networks that may mediate the activation of eosinophils in EoE, we used single-cell regulatory network inference and clustering (SCENIC) to identify gene modules that were coexpressed with transcription factors and enriched for transcription factor cis-regulatory motifs (*16*). Consistent with the analysis of transcriptional pathways, gene modules regulated by nuclear factor κB (NF-κB) subunits, including *NFKB1*, *NFKB2*, *REL*, and *RELB*, were among the most enriched modules in esophagus-resident eosinophils during active disease (fig. S5 and data file S2). NF-κB activation in eosinophils has previously been linked to signaling by the cytokines IL-5 and IL-33, both of which have putative roles in EoE pathogenesis, and has been demonstrated to promote the survival of eosinophils via the suppression of apoptosis (*1*, *4*, *17*–*19*). Gene modules regulated by NF-κB were also elevated in the duodenum during active disease, suggesting that the inflammatory signaling present during active EoE may promote systemic activation of eosinophils, as has been observed in allergic asthma (Fig. 2G) (*20*). Overall, these observations suggest that NF-κB is an important mediator of the activation and survival of eosinophils in EoE and provide insights into the gene regulatory networks active in eosinophils during allergic inflammation.

Phenotypic characteristics and patterns of homing marker expression differentiate esophageal and duodenal T cells

Antigen recognition by allergen-specific T cells is thought to initiate a signaling cascade that leads to the recruitment of eosinophils to the esophagus in EoE (*1*, *4*). To determine the properties of tissue-resident T cells in EoE, we analyzed the subpopulations of T cells present in esophageal and duodenal biopsies. Tissue-specific transcriptional differences caused T cells to segregate in unsupervised analysis by their tissue of origin (fig. S6A). Therefore, we analyzed T cells from the esophagus and duodenum separately. Clustering of these cells revealed six clusters of T cells from each of the esophagus and the duodenum (Fig. 3, A and B, and data file S3). These included clusters resembling $CD8^+$ tissue-resident memory (Trm) cells (clusters E1, E2, and D2), T_H17 cells (E5 and D1), regulatory T (T_{reg}) cells (E3 and D5), peT_H2 cells (E6), natural killer (NK) cells (E4, D3, and D4), and proliferating Ki-67^+ cells (D6) (Fig. 3C). These cluster annotations demonstrated agreement with previously published single-cell RNA sequencing data for innate lymphocytes and NK cells as well as curated modules representing T helper cell phenotypes (fig. S6, B and C, and data file S4) (*21*).

We next analyzed the phenotypic relationships between T cells in the esophagus and duodenum. In general, esophageal T cells exhibited higher levels of activation than those in the duodenum, with esophageal T_H17 cells expressing higher levels of *IL26*, *IL17A*, and *IL17F* and esophageal $CD8^+$ cells expressing higher levels of *IFNG*, *GZMB*, and *GNLY* (fig. S6, D to F, and data file S5). We also found that select homing markers were differentially expressed between esophageal and duodenal T cells. Specifically, T cells from both tissues were broadly positive for *ITGA4* and *ITGB7*, which can combine to form integrin α4β7, a canonical gut homing marker (Fig. 3D) (*22*). In contrast, T cells in the duodenum but not the esophagus expressed *CCR9*, a marker associated with homing to the gut, and only $CD4^+$ T cells in the esophagus expressed *GPR15*, a marker previously associated with homing to the colon or the skin (*23*–*26*). These results suggest that differential expression of these markers may promote the specific homing of T cells to either the esophagus or duodenum. Consistent with this hypothesis, we detected expression of *CCL25* and *C10orf99*, the genes that encode the ligands for CCR9 and GPR15, in only the duodenal epithelium or the esophageal epithelium, respectively (Fig. 3E) (*23*, *24*). Protein expression was confirmed by immunohistochemistry of esophageal biopsies of patients with EoE, which identified GPR15-expressing lymphocytes and GPR15L expression concentrated in the basal epithelium (Fig. 3F). Flow cytometry of T cells from esophageal biopsies derived from an additional set of patients with EoE also demonstrated frequent surface expression of GPR15 on esophagus-resident memory $CD4^+$ T cells (Fig. 3, G and H, and fig. S7, A to C). These results suggest that GPR15 is a previously unidentified marker of esophagus homing that is selectively up-regulated on $CD4^+$ T cells in the esophagus.

peT_H2 cells are enriched in the esophagus during EoE

We next examined the relationship between esophagus-resident T cell clusters and each patient's EoE diagnosis. We found that the relative size of the peT_H2 cluster (E6), calculated as the fraction of total T cells recovered from the esophagus, was significantly higher in patients with active disease (Fig. 4A). The relative size of cluster E6 was also correlated with the frequency of eosinophils detected each patient's esophageal in biopsies, suggesting a relationship between the presence of peT_H2 cells and the recruitment of eosinophils to the esophagus (Fig. 4B).

To further analyze the phenotype of peT_H2 cells in EoE, we identified pathways up-regulated by peT_H2 cells relative to other T cells in the esophagus. Consistent with prior studies of tissue-resident T_H2 cells in EoE and asthma, the pathways significantly up-regulated in peT_H2 cells included arachidonic acid metabolism, lipid metabolism, peroxisome proliferator–activated receptor γ (PPAR-γ) signaling, and eicosanoid production (fig. S8, A and B) (*9*, *27*). To further investigate how dysregulated lipid metabolism may mediate tissue-level inflammation in EoE, we mapped the expression of genes in peT_H2 cells directly onto a network of arachidonic acid metabolism. We identified three genes overexpressed by peT_H2 cells: *PLA2G16*, *PTGS2*, and *HPGDS*, which together can fully process arachidonate stored in membrane-associated phospholipids to form prostaglandin D2 (PGD2) (Fig. 4C). peT_H2 cells also overexpressed the genes for a variety of enzymes involved in the processing of long-chain and very long-chain fatty acids, several of which are reported to have a specificity for arachidonic acid–derived metabolites (*28*–*30*). We also detected these features among peT_H2 cells in a single-cell dataset from a prior study of EoE and datasets generated from skin suction blisters of patients with atopic dermatitis and nasal scrapings of patients with chronic rhinosinusitis (fig. S9) (*9*, *31*, *32*), indicating that they represent functions of peT_H2 cells that are conserved across multiple tissues and disease contexts. These results suggest that a fundamental characteristic of tissue-resident peT_H2 cells across

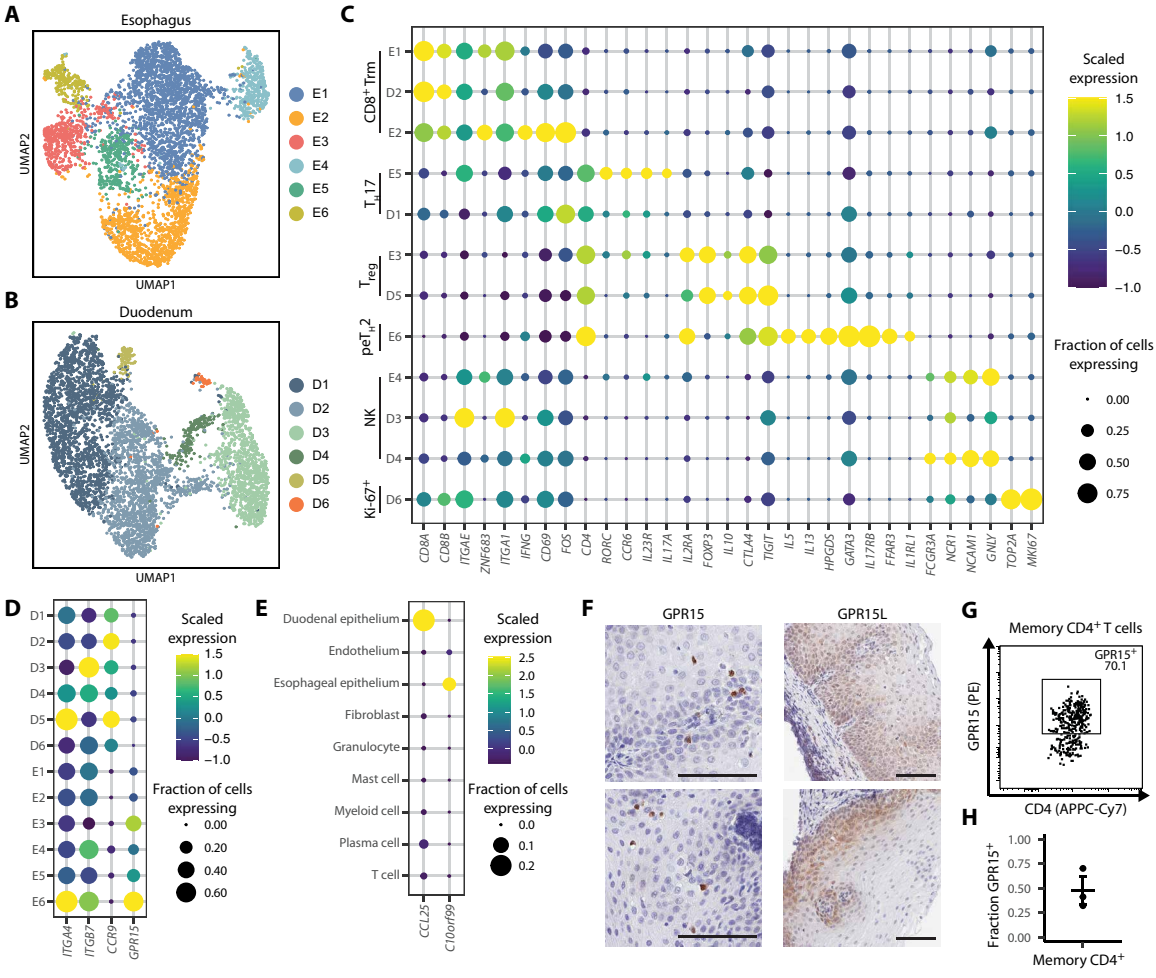

Fig. 3. T cell phenotypes present in the esophagus and duodenum. (**A**) UMAP of T cells recovered from esophageal biopsies colored by phenotypic cluster ($n = 4423$ cells). (**B**) UMAP of T cells recovered from duodenal biopsies colored by phenotypic cluster ($n = 4781$ cells). (**C**) Dot plot of select genes in tissue-resident T cell clusters displaying scaled expression and frequency of expression for each gene. (**D**) Dot plot of select homing markers in T cell clusters from the esophagus and duodenum. (**E**) Dot plot of *CCL25* and *C100rf99*, the ligands for CCR9 and GPR15, in tissue-resident cell phenotypes. (**F**) Immunohistochemical staining for GPR15 and GPR15L in the esophageal biopsies of patients with EoE. Scale bars, 200 μm. Results are representative of $n = 3$ patients. (**G**) GPR15 expression on memory CD4$^+$ T cells isolated from esophageal biopsies of patients with EoE, as measured by flow cytometry. Results are representative of $n = 3$ experiments. (**H**) Fraction of GPR15$^+$ cells among memory CD4$^+$ T cells from esophageal biopsies.

multiple allergic diseases is dysregulation of lipid metabolism conducive to promoting production of PGD2.

To determine to what extent peT$_H$2 cells in the esophagus tissue may directly mediate the recruitment and activation of eosinophils, we performed an analysis of receptor-ligand interactions to predict communication axes present between tissue-resident eosinophils and peT$_H$2 cells. Briefly, we used a permutation-based approach and a database of receptor-ligand interactions to identify receptors selectively expressed on eosinophils that are paired with ligands selectively expressed by peT$_H$2 cells. Predicted interactions between peT$_H$2 cells and eosinophils included those involving the T$_H$2 cytokines IL-13, IL-4, and IL-5 as well as interactions between eicosanoids and the DP2 receptor (*PTGDR2*) (Fig. 4D). Mast cells shared expression of many of these receptors with eosinophils (Fig. 4D), suggesting that similar pathways may mediate the activation of mast cells and eosinophils by peT$_H$2 cells in EoE. Together, these results suggest that a distinguishing characteristic of tissue-resident peT$_H$2 cells in EoE is altered lipid metabolism, which promotes the production of PGD2, and that in addition to T$_H$2 cytokines, PGD2 may play a role in mediating recruitment and activation of eosinophils in the esophagus during EoE.

Tissue-resident peT$_H$2 cells demonstrate a clonally expanded repertoire

We next sought to understand the clonotypic relationships represented among tissue-resident T cell phenotypes. We recovered paired T cell receptor α (TCRα) and TCRβ sequences for individual T cells from nine of the 10 patients in our study (*33*). In sum, we obtained TCRβ sequences for 50.3% of T cells, TCRα sequences for 32.5% of T cells, and both TCRβ and TCRα sequences for 21.5% of T cells (fig. S10A). All subsets of T cells demonstrated some degree of clonal expansion, indicating that these phenotypes include populations of tissue-resident memory T cells (Fig. 5, A to E). Clonally expanded peT$_H$2 cells, defined as multiple cells sharing a common α or β chain

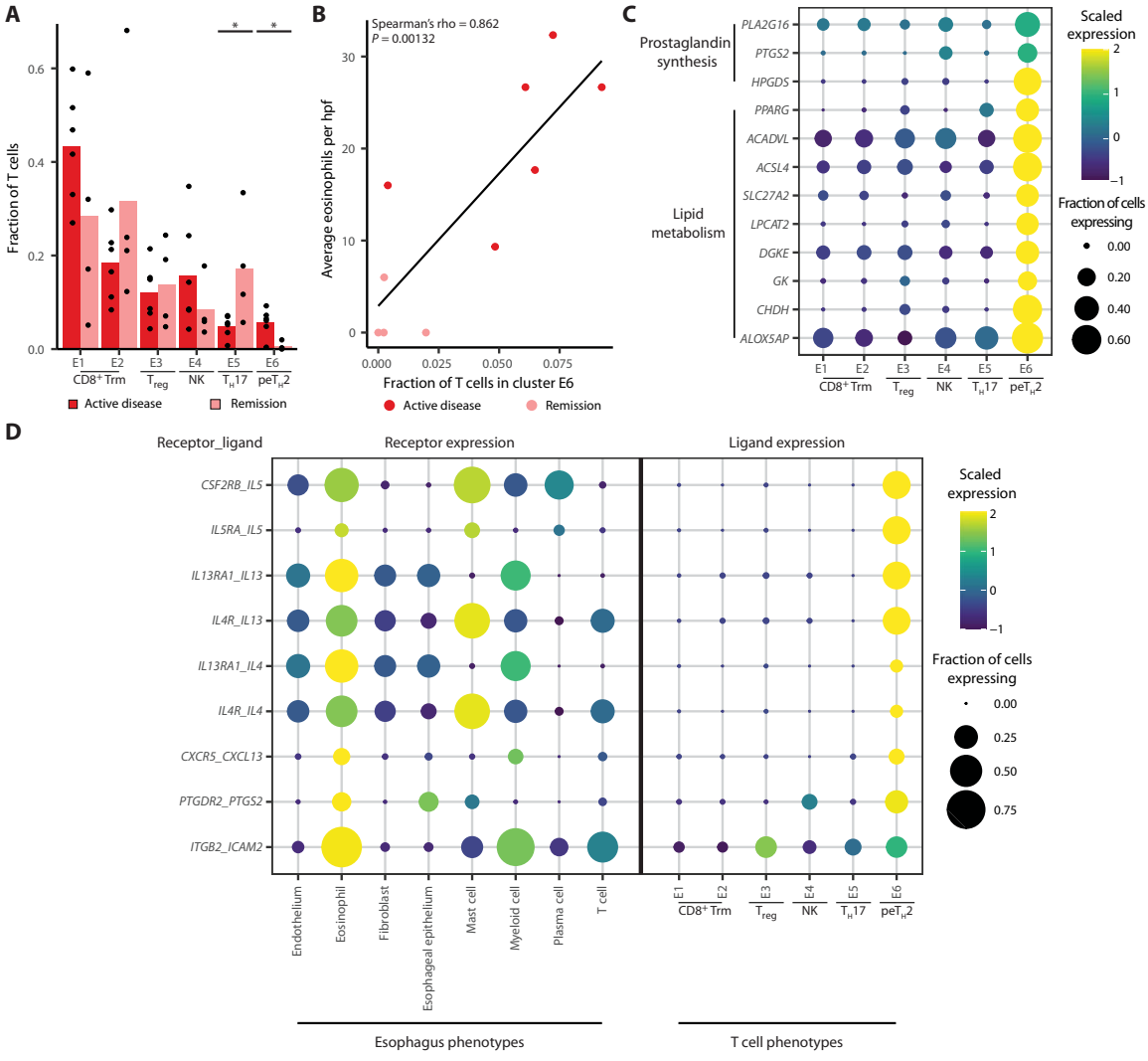

Fig. 4. Properties of peT$_H$2 cells in the esophagus of patients with EoE. (**A**) Relative size of each esophagus T cell cluster by patient and disease status. *P* value was computed using a two-sided Wilcoxon rank sum test (*$P < 0.05$). (**B**) Correlation between fraction of T cells in cluster E6 and number of eosinophils per high-power field (hpf). Spearman's correlation coefficient and the associated *P* value are shown. (**C**) Dot plot showing the expression of genes associated with prostaglandin synthesis or lipid metabolism in each esophagus T cell cluster. (**D**) Ligand-receptor pathway analysis presenting the expression of receptors and ligands in pathways determined to be selectively up-regulated between eosinophils and peT$_H$2 cells. All pathways shown are determined to be statistically significant (Materials and Methods).

complementarity-determining region 3 (CDR3) sequence, were detected in three of the four patients with active disease from whom multiple TCRs were recovered from the peT$_H$2 cluster (Fig. 5F). These results indicate that the repertoire of tissue-resident peT$_H$2 cells in EoE exhibits clonal expansion, an important feature of an antigen-specific response.

Peripheral CRTH2$^+$CD161$^+$ T cells are enriched for a peT$_H$2 phenotype

The surface marker CD161 has been reported to be up-regulated on highly differentiated peT$_H$2 cells in allergy and helminth infection, and peripheral CRTH2$^+$CD161$^+$ memory CD4$^+$ T cells have been associated with EoE (*8*, *34*, *35*). To understand to what extent the peT$_H$2 phenotype observed in the esophagus of patients with active EoE is recapitulated among peripheral CRTH2$^+$CD4$^+$ T cells, we obtained peripheral blood mononuclear cells (PBMCs) from eight of the patients in this study. From these samples, we isolated memory CD4$^+$ T cells and polyclonally activated these cells ex vivo in a TCR-dependent manner (anti-CD3/anti-CD28 coated beads) for 6 hours. We then separated three populations of memory CD4$^+$ T cells: CRTH2$^+$CD161$^+$, CRTH2$^+$CD161$^-$, and CRTH2$^-$CD161$^-$ by fluoresence activated cell sorting (FACS) (Fig. 6A). Compared with patients in remission, patients with active disease had significantly higher frequencies of CRTH2$^+$CD161$^-$ cells and a trend toward increased frequencies of CRTH2$^+$CD161$^+$ cells (Fig. 6B).

We also processed CRTH2$^+$CD161$^+$, CRTH2$^+$CD161$^-$, and CRTH2$^-$CD161$^-$ CD4$^+$ T cells sorted from these eight patients for single-cell RNA sequencing. We obtained data from a total of 30,635 cells, comprising 6664 CRTH2$^+$CD161$^+$ cells, 7597 CRTH2$^+$CD161$^-$ cells, and 16,374 CRTH2$^-$CD161$^-$ cells. Among these cells, we identified six major clusters representing phenotypic states among these CD4$^+$ T cells in the peripheral blood (Fig. 6, C and D, and data file S6). The CRHT2$^+$CD161$^-$ population was enriched for cells in cluster 2, and the CRTH2$^+$CD161$^+$ population

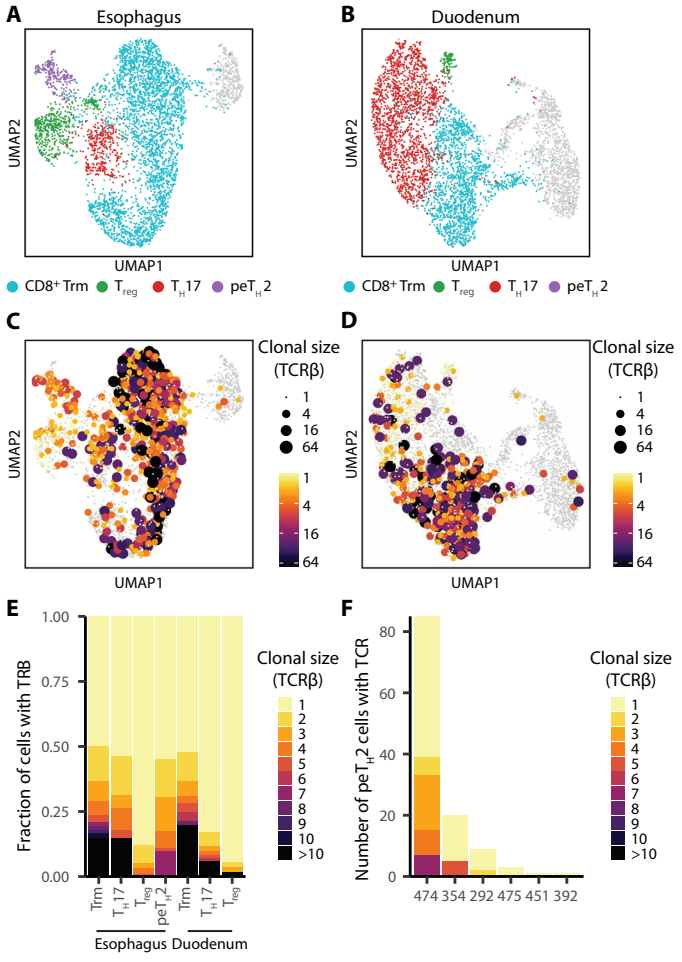

Fig. 5. Clonotypic relationships of T cells in the esophagus and duodenum. (**A**) UMAP of phenotypes present among esophageal T cells and (**B**) duodenal T cells. (**C**) Clonal size of esophageal T cells and (**D**) duodenal T cells mapped onto corresponding UMAPs. Clonal size is defined as the number of cells from a given patient that share a given TCRβ sequence. (**E**) Stacked bar plot of clonal size of each phenotype. (**F**) Bar plot of clonal size of peTH2 cells in each patient.

was enriched for cells in clusters 2 and 3 (Fig. 6E). These clusters did not completely align with the CRTH2$^+$CD161$^-$ and CRTH2$^+$CD161$^+$ populations defined by FACS, indicating a degree of transcriptional heterogeneity within each population defined by surface protein expression. Clusters 2 and 3 expressed features typically associated with TH2 cells, including the cytokines *IL4* and *IL13* (Fig. 6F). Cluster 3, however, expressed the highest levels of the TH2 cytokines *IL4*, *IL5*, *IL9*, and *IL13* as well as other features previously associated with a peTH2 phenotype, including high levels of *HPGDS* and the transcripts for surface markers *IL17RB* and *IL1RL1* (*8*, *34*). Together, these data suggest that cluster 2 contained conventional TH2 (convTH2) cells and cluster 3 contained peTH2 cells.

We then analyzed the expression of genes associated with tissue-resident peTH2 cells in each cluster. We found that peripheral peTH2 cells, but not convTH2 cells, up-regulated the expression of the genes associated with dysregulated lipid metabolism identified in esophagus-resident peTH2 cells (Fig. 6F). Although the levels of TH2 cytokines were higher among peripheral peTH2 cells, the levels of these lipid metabolism–related genes were higher among tissue-resident peTH2 cells, suggesting that dysregulated lipid metabolism and eicosanoid synthesis is an acquired function of peTH2 cells in esophageal tissue.

Peripheral convTH2 and peTH2 cells are clonally expanded and demonstrate convergence of TCR sequences

To assess the clonotypic relationships among peripheral CRTH2$^+$CD4$^+$ T cells in EoE, we recovered paired TCRα and TCRβ sequences from sorted cells (fig. S10B). We found high levels of clonal expansion among both convTH2 and peTH2 cells but not non-TH2 cells, suggesting that these cells may be expanded by exposure to antigen during active disease (Fig. 7, A and B). To determine to what extent cells within a clonotype may share similar phenotypes, we examined the distribution of phenotypes present within each expanded clonotype. We found that nearly all expanded clonotypes demonstrated a preference for either the convTH2 phenotype or the peTH2 phenotype, indicating that these phenotypes represent distinct clonal lineages, potentially associated with the recognition of distinct epitopes, which may diverge because of distinct conditions experienced during priming (Fig. 7C). We also found that the diversity of TCRβ sequences among the peTH2 and convTH2 populations was significantly less than non-TH2 cells, further indicating that these phenotypes are associated with expanded T cell clonotypes (Fig. 7D).

We sought to determine to what extent distinct TCR clonotypes among the convTH2 and peTH2 populations may recognize common epitopes. We determined the nearest neighbor Hamming distances for all TCRβ CDR3 amino acid sequences recovered from each patient and found that clonotypes in the convTH2 and peTH2 populations were significantly more likely than non-TH2 cells to have a nearest neighbor within a Hamming distance of one, corresponding to a single amino acid substitution, demonstrating a convergence of TCR sequences among these clonotypes (Fig. 7E). We also used grouping of lymphocyte interactions by paratope hotspots analysis, which defines "specificity groups" of TCRs that are predicted to share a common epitope (*36*). convTH2 and peTH2 cells clonotypes were significantly more likely than non-TH2 cells to belong to a specificity group with another TCRβ sequence, further indicating that distinct clonotypes among these populations likely share common epitopes (Fig. 7F). In addition, we observed that clonotypes that had a nearest neighbor Hamming distance of one or belonged to a GLIPH2 specificity group were more expanded than clonotypes without these characteristics, suggesting a dominant oligoclonal antigen-specific response (fig. S11, A and B). Trends in clonal expansion, diversity, and TCR sequence convergence were more pronounced between the transcriptionally defined convTH2 and peTH2 clusters than the protein-defined CRTH2$^+$CD161$^-$ and CRTH2$^+$CD161$^+$ fractions obtained with FACS, indicating that the CD161 marker is neither completely sensitive nor specific for the clonally expanded peTH2 transcriptional state (fig. S11, C to F). Overall, these results indicate that peripheral convTH2 and peTH2 cells in patients with EoE exhibit substantial clonotypic expansion and TCR sequence convergence, suggesting that their repertoire is selected for a defined set of epitopes.

Esophagus-resident peTH2 clonotypes are present among peripheral CRTH2$^+$CD4$^+$ cells and up-regulate *GPR15*

To determine whether T cell clonotypes were shared among peripheral peTH2 cells and esophagus-resident peTH2 cells, we compared TCR usage between peTH2 cells from esophageal tissue and cells from

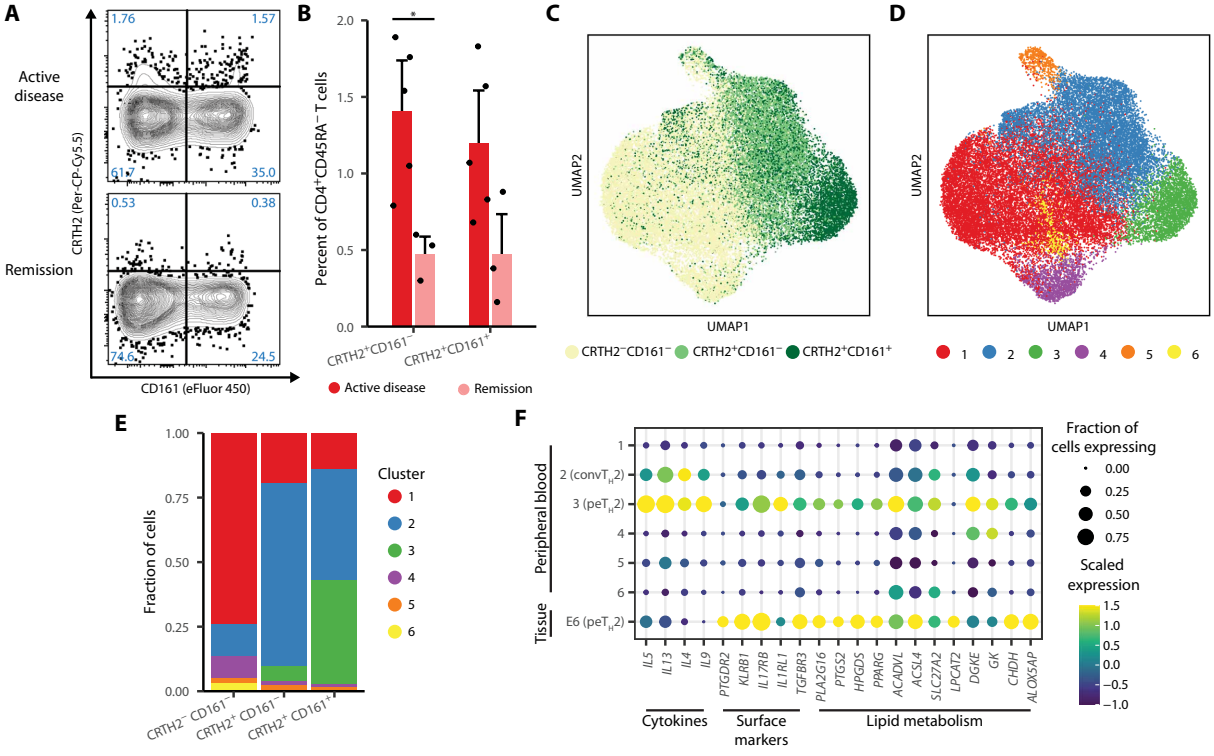

Fig. 6. Comparisons between peripheral and esophagus-resident peTH2 phenotypes. (**A**) Representative staining of CRTH2 and CD161 from peripheral blood of patients with EoE in disease or remission. (**B**) Percentage of CRTH2$^+$CD161$^+$ and CRTH2$^+$CD161$^-$ among memory CD4$^+$CD45RA$^-$ T cells, as determined by flow cytometry. *P* values are calculated using a one-sided Wilcoxon rank sum test (*$P < 0.05$). (**C**) UMAP of sorted CRTH2-CD161$^-$, CRTH2$^+$CD161$^-$, and CRTH2+CD161$^+$ cells colored by sort fraction ($n = 30{,}635$ cells; eight patients). (**D**) UMAP of sorted cells colored by phenotypic cluster. (**E**) Distribution of phenotypic clusters within each sort fraction. (**F**) Dot plot of peTH2-associated genes in T cells from peripheral blood CD4$^+$ T cells and cluster E6 from esophageal biopsies.

peripheral blood. We found a total of 26 cells from two patients that expressed a TCRβ or TCRα sequence that was also detected in an esophagus-resident peTH2 cell, indicating that esophagus-resident peTH2 clonotypes can simultaneously be detected in the tissue and among CRTH2$^+$CD4$^+$ cells in the peripheral blood (Fig. 7G). The TCRβ CDR3 sequences of two of these clonotypes from the same patient differed by only a single amino acid substitution (Gly ➔ Ser), suggesting that these two esophagus-trafficking peTH2 clonotypes likely recognized the same epitope. In total, 84.6% (22 of 26) of peripheral cells that belonged to clonotypes detected among esophagus-resident peTH2 cells had a peTH2 phenotype, indicating that a subset of peripheral peTH2 cells share both phenotypic and clonotypic identity with esophagus-resident peTH2 cells.

To determine whether any phenotypic characteristics distinguish esophagus-associated peTH2 cells from other peTH2 cells in peripheral blood, we identified genes that were differentially expressed between the two populations. The gene *GPR15* was the most significantly up-regulated transcript in peTH2 clonotypes that were found in the esophagus tissue (Fig. 7H and data file S7). Only 1.04% of all peripheral peTH2 cells had detectable *GPR15* transcript expression, but *GPR15* transcript was detected in 23% (6 of 26) of peripheral peTH2 clonotypes that were also detected in esophageal biopsies (fig. S12, A and B). This result suggests that GPR15 may function to promote trafficking of peTH2 cells to the esophagus during EoE and that GPR15 may serve as a marker of esophagus-associated peTH2 cells in the peripheral blood of patients with EoE.

peTH2 cells from patients with milk-triggered EoE demonstrate milk reactivity

Last, to determine to what extent esophagus-homing peTH2 cells in EoE are reactive to disease-associated antigens, we obtained PBMCs from nine patients with EoE having milk-triggered disease. We stimulated the cells for 22 hours with milk protein and analyzed the cells using flow cytometry (fig. S13A). The activation marker CD154 (CD40L) was used to detect antigen-reactive CD4$^+$ T cells (*37*). Antigen-reactive CD154$^+$ T cells were significantly enriched for CRTH2$^+$CD161$^+$ cells relative to resting CD154$^-$ cells, indicating that a substantial fraction of peripheral peTH2 cells from patients with EoE are reactive to food antigens (Fig. 7, I and J, and fig. S13B). In addition, GPR15 was enriched on CD154$^+$ T cells relative to CD154$^-$ T cells and was expressed on a fraction of CD154$^+$CRTH2$^+$CD161$^+$ T cells, suggesting that a subset of antigen-reactive peTH2 cells may have enhanced esophagus homing potential (Fig. 7, I and K, and fig. S13B). Free fatty acid receptor 3 (FFAR3), a previously reported marker for peTH2 cells in EoE (*9*), was also enriched on CD154$^+$ cells relative to CD154$^-$ cells but was detected on a lower fraction of memory CD4$^+$ cells than was GPR15 (fig S13C). Overall, these results demonstrate that a significant fraction of peTH2 clonotypes are reactive to disease-associated food antigens and confirm the association of GPR15 with antigen-reactive peTH2 cells in EoE.

DISCUSSION

Here, we have analyzed the transcriptional characteristics and TCR repertoire of peTH2 cells from the esophageal biopsies, duodenal

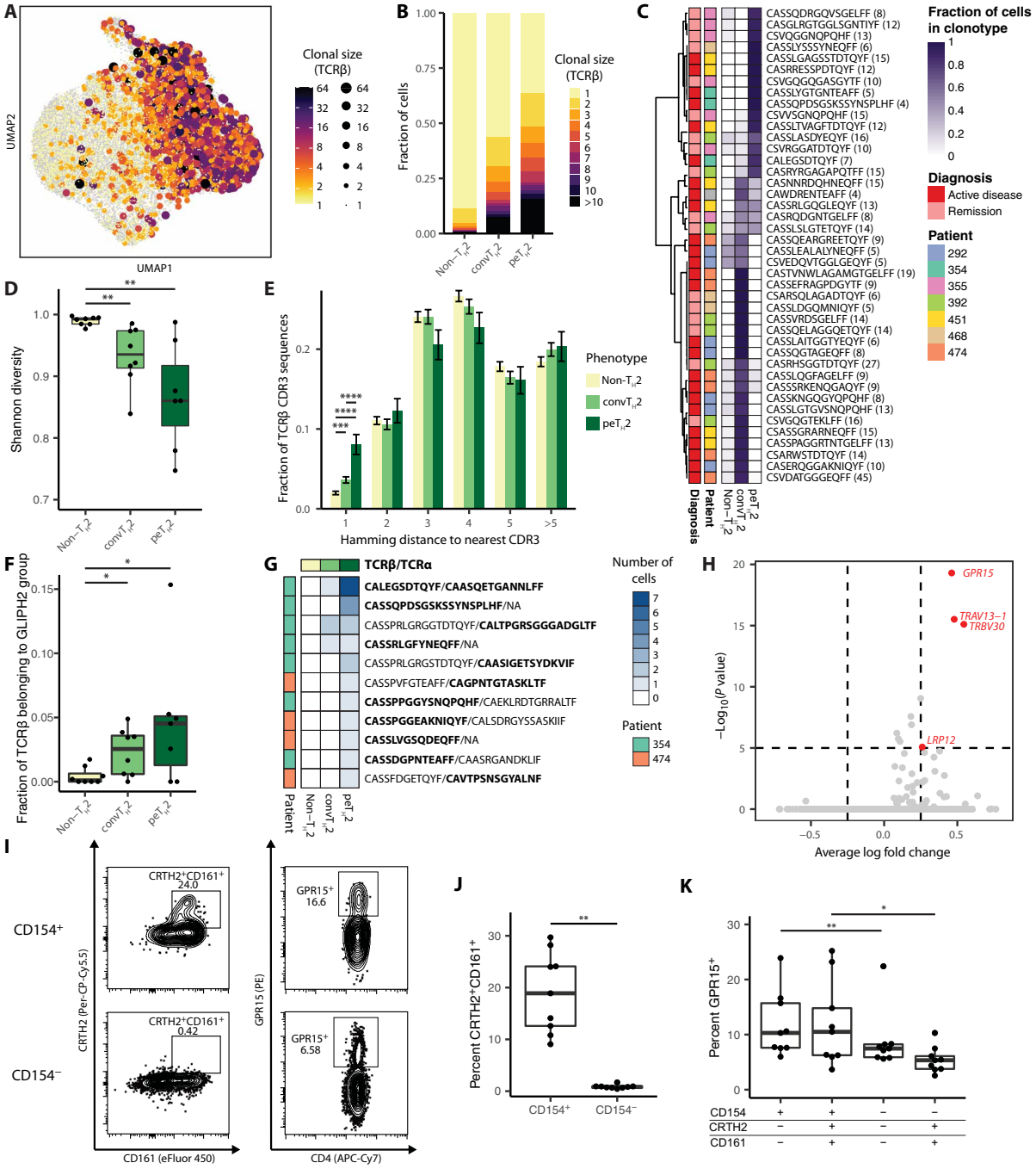

Fig. 7. TCR repertoire of peripheral convT$_H$2 and peT$_H$2 cells. (**A**) Clonal size, calculated using TCRβ, overlaid on UMAP. (**B**) Distribution of clonal size among non-T$_H$2, convT$_H$2, and peT$_H$2 phenotypes. (**C**) Distribution of non-T$_H$2, convT$_H$2, and peT$_H$2 phenotypes within expanded clonotypes. Up to the seven most expanded clonotypes recovered from each patient are displayed, provided that they consist of greater than three cells. The heatmap is colored according to fraction of cells in that clonotype with a given phenotype. (**D**) Shannon diversity of non-T$_H$2, convT$_H$2, and peT$_H$2 cells. Samples with fewer than 10 TCRβ sequences recovered are excluded. *P* values are calculated using a two-sided Wilcoxon rank sum test (**$P < 0.01$). (**E**) Distribution of nearest-neighbor Hamming distance between CDR3 sequences in each phenotype. *P* values are calculated using a two-sided chi-squared proportion test (***$P < 0.001$ and ****$P < 0.0001$). (**F**) Fraction of TCRβ sequences in each phenotype that are related to another TCRβ sequence from the same patient by GLIPH2. Samples with fewer than 10 TCRβ sequences recovered are excluded. *P* values are calculated by a one-sided Wilcoxon rank sum test (*$P < 0.05$). (**G**) peT$_H$2 clonotypes shared between the peripheral blood and the esophagus. Heatmap presents the distribution of phenotypes present in peripheral blood for each clonotype. Sequences highlighted in bold were shared between the esophagus and peripheral blood; other sequences are paired with these sequences in either location. (**H**) Genes up-regulated by clonotypes detected in esophagus tissue relative to all other peripheral peT$_H$2 cells. *P* values are calculated using a two-sided Wilcoxon rank sum test and are adjusted with Bonferroni correction. (**I**) Representative staining of CD154$^+$ and CD154$^-$ memory CD4$^+$ T cells from patients with milk-triggered disease. (**J**) Frequency of CRTH2$^+$CD161$^+$ cells among CD154$^+$ and CD154$^-$ cells after culture with milk antigen. *P* values were calculated using a paired two-sided Wilcoxon rank sum test (**$P < 0.01$) (**K**) Frequency of GPR15$^+$ cells among memory T cell subsets after culture with milk antigen. *P* values were calculated using a paired two-sided Wilcoxon rank sum test (*$P < 0.05$ and **$P < 0.01$).

biopsies, and peripheral blood of patients with EoE. By comparing the characteristics of peT$_H$2 cells across these three compartments, we provide insight into the mechanisms that drive inflammation in EoE, including the pathways that lead to recruitment of peT$_H$2 cells to the esophagus, the abilities of these cells to mediate eosinophilic inflammation, and the clonal relationships manifested among this population.

Previous single-cell sequencing–based studies have been limited in their ability to detect eosinophils and other granulocytes because of their low RNA content and high concentration of ribonucleases (*32*). Using Seq-Well, we recovered numbers of eosinophils that correlated with their counts in clinical biopsies. We found that esophagus-resident eosinophils exhibited enhanced expression of genes regulated by NF-κB, indicating that these cells are likely responsive to inflammatory signals produced in EoE and are active mediators of inflammation. Activation of NF-κB in eosinophils has been demonstrated to increase eosinophil survival and has been associated with IL-5 and IL-33 signaling (*17*–*19*), providing mechanistic insight into the pathways influencing the activation of eosinophils during EoE.

In this study, we found expression of the marker *GPR15* to be specifically enriched on CD4$^+$ cells in the esophagus, especially on peT$_H$2 cells. *GPR15* expression was also increased on peT$_H$2 clonotypes in the peripheral blood that were also detected in esophageal tissue and was found to be up-regulated on milk-reactive peT$_H$2 cells in patients with milk-triggered disease. These data suggest that GPR15 expression promotes esophagus homing of peT$_H$2 cells in EoE and that GPR15 may serve as a marker for esophagus-trafficking peT$_H$2 cells in the peripheral blood of patients with EoE. Further investigation of this finding in increased numbers of patients with a range of clinical presentations could enhance understanding of how this population influences the pathology of EoE.

We have also demonstrated the existence of clonal expansion among peT$_H$2 cells in both the esophagus tissue and the periphery. In addition, we detected expanded clonotypes that exhibit convergence of TCR sequences. This observation suggests the presence of an oligoclonal response by multiple clonotypes that adopt a shared phenotype and may be dominated by a small number of epitopes within a patient. Clonotypes typically demonstrated a preference for one of the peT$_H$2 or convT$_H$2 transcriptional states, suggesting that each phenotype represents a distinct set of clonal lineages that may diverge because of the nature of the particular antigens recognized or because of distinct conditions experienced during priming. Last, we found that the peT$_H$2 phenotype is highly enriched among milk-reactive T cells in patients with milk-triggered disease, further suggesting that the dominant epitopes recognized by peT$_H$2 cells in EoE are derived from disease-associated allergens. Future studies involving the validation of allergen-specific peT$_H$2 cells in patients with EoE could enable the identification of the precise allergen-derived epitopes recognized by peT$_H$2 cells in EoE and allow the diagnosis of EoE-related food triggers without empirical evaluation of avoidance diets, a significant unmet clinical need.

peT$_H$2 cells were originally described as a pro-eosinophilic subset of T$_H$2 cells distinct from convT$_H$2 cells with an enhanced ability to produce the cytokine IL-5 (*38*, *39*). Additional characteristics of peT$_H$2 cells have been proposed across a wide spectrum of allergic diseases, including increased expression of the surface markers CD161, IL-25R, IL-33R, CCR8, and FFAR3; the enzyme HPGDS; and the transcription factor PPAR-γ (*8*, *9*, *34*, *40*, *41*). In this study, we have highlighted previously undescribed characteristics associated with this phenotype, including an up-regulation of genes associated with lipid metabolism and expression of a complete synthetic pathway for the eicosanoid PGD2. Our analysis of cognate receptor-ligand pairings transcriptionally active in the esophageal tissue (Fig. 4D) predicts that peT$_H$2 cells directly influence tissue-resident eosinophils through the production of PGD2, a function that was also detected in peripheral peT$_H$2 cells but not convT$_H$2 cells. These findings suggest that the pathogenicity of peT$_H$2 cells may result directly from their production of PGD2 and motivates further studies analyzing the differentiation and behavior of peT$_H$2 cells. Such studies could inform mechanisms and interventional treatments for EoE and for other allergic disorders. In addition, EoE is a reported adverse event for patients undergoing oral immunotherapy (OIT) for food allergy (*42*–*44*), suggesting that similar characteristics may develop among food allergen–specific CD4$^+$ T cells in patients undergoing OIT.

Allergen-induced inflammation in EoE has been suggested to be driven by the recognition of antigen by peT$_H$2 cells (*1*, *4*). This hypothesis is further supported by the detection of clonal expansion and convergence of TCR sequences among tissue-resident and peripheral peT$_H$2 cells in this study. We observed that these peT$_H$2 cells express the cytokines IL-5 and IL-13, which promote inflammation in EoE by driving eosinophil recruitment and contributing to epithelial barrier dysfunction, respectively (*1*, *4*, *5*). In addition, we report evidence that esophagus-resident peT$_H$2 cells are also involved in the production of PGD2. The release of PGD2 may promote inflammation by generating a positive feedback loop involving the chemotaxis and activation of eosinophils, mast cells, and peT$_H$2 cells themselves. This positive feedback loop may be further amplified by other inflammatory signals such as IL-33 release from damaged epithelial cells, which induces further activation of *IL1RL1*-expressing eosinophils and peT$_H$2 cells. In addition to these factors, group 2 innate lymphoid cells (ILC2s), which have also been observed in the esophageal biopsies of patients with EoE (*45*), may contribute to inflammation in EoE through the production of IL-5 and IL-13. We did not detect ILC2s in our single-cell RNA sequencing; this absence may have resulted from the rarity of these cells combined with the relatively small biopsies available in this study.

In summary, we have profiled key allergic mediators present in the esophageal and duodenal biopsies of patients with EoE, including tissue-resident eosinophils and peT$_H$2 cells. We find that tissue-resident peT$_H$2 cells are a clonally expanded population associated with a distinct phenotypic state involving eicosanoid signaling. These cells are enriched among food allergen–reactive CD4$^+$ T cells in patients with EoE and exhibit an up-regulation of GPR15, which promotes esophagus homing. Further knowledge of the development of peT$_H$2 cells, their interactions with other allergic mediators, and the antigens recognized by these cells is vital to advancing our understanding, diagnosis, and treatment of EoE and other allergic and eosinophilic diseases.

MATERIALS AND METHODS

Study design

The objective of this study was to understand the types and functions of cells present in esophageal biopsies and peripheral blood of patients with EoE and to determine how these cells are altered in active disease versus remission. Cells from tissue biopsies and peripheral blood were analyzed with paired single-cell RNA and TCR

sequencing as well as flow cytometry. The study was approved by the Institutional Review Board of Partners HealthCare (protocol nos. 2010P002087 and 2011P001159) at Massachusetts General Hospital. Sample size was determined on the basis of the availability of biopsy samples. Researchers performing the single-cell RNA sequencing and flow cytometry experiments were blinded to the patient diagnoses. Diagnoses of active EoE and EoE in remission were provided by physicians and considered factors such as the number of eosinophils per high-power field and other features of microscopic pathology, as well as the appearance of the esophagus upon endoscopy, as assessed by EoE Endoscopic Reference Score (EREFS) scoring (*46*), and current patient symptoms (table S1).

Esophagus biopsy collection and processing

Up to six biopsies in total from the proximal, medial, and distal esophagus or duodenum were collected from each patient. Biopsies were cut with scalpels into fragments of ~1 mm^2 and processed into a single-cell suspension by performing two subsequent digestions with collagenase A (2 mg/ml) and deoxyribonuclease I (100 μg/ml) (both from MilliporeSigma, St. Louis, MO) in RPMI 1640 medium (Gibco, Waltham, MA) for 40 min at 37°C. Remaining fragments of tissue were removed by centrifugation (100*g* for 2 min), and the supernatant cell suspension was filtered through a 70-μm cell strainer and washed twice with cold staining buffer (phosphate-buffered saline + 0.5% bovine serum albumin + 2 mM EDTA) before further use. For analysis of biopsy samples with flow cytometry, single-cell suspensions from multiple patients were pooled and labeled with BUV395-conjugated anti-CD3 (clone UCHT1), allophycocyanin-Cy7 (APC-Cy7)–conjugated anti-CD4 (RPA-T4), and phycoerythrin (PE)-Cy7–conjugated anti-CD45RA (HI100) (all from BD Biosciences, San Jose, CA); LIVE/DEAD Fixable Blue stain (L23105; Thermo Fisher Scientific, Waltham, MA); and PE-conjugated anti-GPR15 (SA302A10; BioLegend, San Diego, CA). Samples were analyzed with a BD LSRFortessa X-20 instrument (BD Biosciences), and the data were analyzed with FlowJo v10 software.

Activation and sorting of peripheral blood T cell populations

Cryopreserved PBMC from 8 of the 10 patients included in the tissue-resident single-cell analysis were thawed, and memory $CD4^+$ T cells were isolated with the EasySep Human Memory $CD4^+$ T Cell Enrichment Kit (STEMCELL Technologies, Vancouver, BC, Canada). T cells were cultured in AIM-V medium (Gibco) for 6 hours at a density of 2×10^6 in 0.5 ml of medium per well in 48-well plates, with human T-Activator CD3/CD28 beads (Thermo Fisher Scientific) in a 1:3 ratio of beads to T cells. After harvesting, the cells were labeled with BUV395-conjugated anti-CD3, APC-Cy7–conjugated anti-CD4, PE-Cy7–conjugated anti-CD45RA, peridinin-chlorophyll-protein (PerCP)-Cy5.5–conjugated anti-CRTH2 (BM16; BD Biosciences), eFluor 450–conjugated anti-CD161 (HP-3G10; Thermo Fisher Scientific), and LIVE/DEAD Fixable Blue stain. Live $CD3^+CD4^+CD45RA^-$ $CRTH2^+CD161^+$, $CRTH2^+CD161^-$, and $CRTH2^-CD161^-$ T cells were sorted with a FACSAria Fusion instrument (BD Biosciences).

Analysis of peripheral blood milk-reactive $CD4^+$ T cells

Cryopreserved PBMCs from nine patients with milk- or dairy-triggered EoE (no overlap with the patients included in the single-cell analysis) were thawed and cultured in AIM-V medium for 22 hours, with or without cow's milk protein (75 μg/ml; M7409; MilliporeSigma), at a density of 5×10^6 in 1 ml of medium per well in 24-well plates. Fluorescein isothiocyanate (FITC)–conjugated anti-CD154 (clone TRAP1; BD Biosciences) was added to the cultures (20 μl per well) for the last 3 hours. After harvesting, the cells were labeled with BUV395-conjugated anti-CD3, APC-Cy7–conjugated anti-CD4, PE-Cy7–conjugated anti-CD45RA, FITC-conjugated anti-CD154, PerCP-Cy5.5–conjugated anti-CRTH2, eFluor 450–conjugated anti-CD161, PE-conjugated anti-GPR15, APC-conjugated anti-FFAR3 (LS-C214200; LSBio, Seattle, WA), and LIVE/DEAD Fixable Blue stain. Flow cytometry data were collected with a FACSAria Fusion instrument and analyzed with FlowJo v10 software.

Single-cell RNA sequencing

Single-cell suspensions from esophageal biopsies, duodenal biopsies, and sorted subsets of peripheral blood $CD4^+$ memory T cells were processed for single-cell RNA sequencing using the Seq-Well platform with second-strand chemistry, as previously described (*10*, *11*). Libraries were barcoded and amplified using the Nextera XT Kit (Illumina, San Diego, CA) and were sequenced on a NovaSeq 6000 (Illumina).

Paired single-cell TCR sequencing and analysis

Paired TCR sequencing and read alignment were performed as described by Tu *et al.* (*33*). Briefly, whole-transcriptome amplification product for each sample was enriched for TCR transcripts using biotinylated probes for the human *TRAC* and *TRBC* regions and magnetic streptavidin beads. The enriched product was further amplified using human V region primers and Nextera sequencing handles. Libraries were then sequenced on an Illumina MiSeq or NextSeq using single-end reads. CDR3 consensus sequences were aligned as outlined previously. To prevent collisions between cell barcodes that may originate from Hamming distance correction, we aggregated all molecules with the same CDR3 sequence, clustered the unique molecular identifiers (UMIs) of these sequences according to Hamming distance with a maximum distance of 2, and retained the single UMI with the greatest number of total reads. UMIs with less than an 80% CDR3 consensus frequency were then excluded from analysis. GLIPH2 analysis was performed as described by Huang *et al.* (*36*) using the default parameters and version 2 of the provided reference for human data.

Single-cell data processing and visualization

Raw read processing of single-cell RNA sequencing reads was performed according to the work of Macosko *et al.* (*47*). Briefly, reads were aligned to the hg38 reference genome and collapsed by cell barcode and UMI. For the dataset generated from esophageal and duodenal biopsies, cells with less than 500 unique genes detected and genes detected in fewer than five cells were filtered out, and for the dataset of peripheral $CD4^+$ memory T cells, cells with less than 900 unique genes detected and genes detected in fewer than five cells were filtered out. First, the data for each cell were log-normalized to account for library size. We then selected variable genes with log-mean expression values greater than 0.1 and a dispersion of greater than 1. The ScaleData function in Seurat was used to regress out the number of UMI and percentage of mitochondrial genes in each cell and to scale the data to unit variance using a Poisson model. Next, principle components analysis (PCA) was performed, and the top 10 components were used to generate a UMAP visualization. Clusters were determined using the FindClusters function in Seurat. A small

number of cells recovered from esophageal biopsies clustered with duodenal epithelial cells and were excluded from further analysis.

Correction for ambient RNA contamination using SoupX

Ambient RNA correction was performed using SoupX v0.3.0 as described by Young and Behjati (*48*) with minor modifications. Cell contamination fractions were estimated using the genes *KRT4*, *KRT5*, *KRT13*, *KRT15*, and *KRT6A* in non-esophageal epithelial cells for samples from the esophagus and the genes *IGHA1*, *IGHA2*, *IGHM*, *IGJ*, and *IGKC* in non-plasma cells for samples from the duodenum. These estimates were refined using the calculateContaminationFraction to fit lowess curves between the number of UMI for each cell and the estimated contamination fraction. Adjusted counts were rounded to integers to preserve the count nature of the data. After ambient RNA correction was complete, the data were reprocessed and revisualized as described above.

Doublet removal and individual cell type analysis

Clusters representing a single-cell type were first processed as described in the "Single-cell data processing and visualization" section above. Doublet clusters were then identified as clusters that strongly expressed marker genes associated with more than one cell population and were discarded. Preprocessing steps were then performed one additional time before beginning analysis.

Gene module and pathway enrichment analysis

Gene sets for innate T cell subsets and NK cells were generated by determining the top 30 differentially expressed genes by each subset in the data from Gutierrez-Arcelus *et al.* (*21*), were obtained from Molecular Signatures Database (MSigDB) (*49*), or were curated according to standard marker genes for T helper cells. Gene scores were obtained using the AddModuleScore function in Seurat. For analysis of eosinophil transcriptomes, MSigDB pathways in the Hallmarks collection were analyzed, and for analysis of peT_H2 cells, MSigDB pathways in the Kyoto Encyclopedia of Genes and Genomes and BioCarta collections were analyzed.

SCENIC analysis of eosinophils

The Python package pySCENIC version 0.9.18 was used to infer gene regulatory networks in eosinophils (*16*, *50*). The input into the pySCENIC workflow was the gene count matrix for cells classified as eosinophils and the RcisTarget database containing transcription factor motif scores for gene promoters around transcription start sites in the hg38 genome. Transcription factor modules up-regulated in eosinophils during active disease were identified by performing a two-sided Wilcoxon rank sum test on the AUCell scores for each transcription factor module between eosinophils from esophageal biopsies of patients with active disease and eosinophils from the duodenal biopsies of all patients.

Immunohistochemical staining

Formalin-fixed paraffin-embedded biopsy sections were prepared using standard protocols. Heat-mediated epitope retrieval was performed at 97°C for 20 min with pH 6 citrate buffer, using the Thermo Fisher Scientific PT module. Slides were run on the Thermo Fisher Scientific 360 AutoVision immunohistochemistry stainer. The run consisted of the following: endogenous peroxidase blocking, 10 min; protein block, 30 min; primary antibody, 60 min; labeled polymer, 30 min; and 3,3′-diaminobenzidine (DAB), 5 min. The primary antibodies used were GPR15 (HPA-013775; MilliporeSigma) and C10orf99 (PA5-62266; Thermo Fisher Scientific).

Receptor-ligand pathway analysis

To identify receptor-ligand interactions between peT_H2 cells and eosinophils in the esophagus tissue, we used pathways annotated as "known" and "literature supported" from a published database of receptor-ligand pairs (*51*). We aimed to identify receptor-ligand pairs in which the receptor was selectively up-regulated on eosinophils relative to other cells from esophageal biopsies, and the ligand was selectively up-regulated by peT_H2 cells relative to other T cell subsets. We defined eosinophils or peT_H2 cells as "expressing" a receptor or ligand if at least 10% of the cells in that cluster expressed transcript for that receptor or ligand. For all pathways in which both eosinophils and peT_H2 cells expressed the corresponding receptor and ligand, we then defined a "receptor score" and "ligand score" equal to average normalized expression value for the gene encoding the receptor or ligand. We then generated a null distribution for receptor scores and ligand scores by performing 10,000 permutations of the cell type labels among cells recovered from esophageal biopsies and recalculating both receptor scores and ligand scores. We then used this null distribution to calculate *P* values for both receptor scores and ligand scores and defined the *P* value for each receptor-ligand pair as the maximum of the *P* value for the receptor score and the *P* value for the ligand score.

Reanalysis of literature datasets

Data from the work of Wen *et al.* (*9*), Bangert *et al.* (*31*), and Ordovas-Montanes *et al.* (*32*) were obtained from GSE126250 and GSE153760 and the supplementary data of Ordovas-Montanes *et al.* For Bangert *et al.* (*31*), data from skin suction blisters of patients with atopic dermatitis were used. For all datasets, non–T cells and T cells with under 500 unique genes detected were excluded. Data from the work of Bangert *et al.* and Ordovas-Montanes *et al.* were processed using the methodology described above. Data from Wen *et al.* were first normalized by computing transcripts per million. Variable genes were then selected using the FindVariableGenes function in Seurat and scaled using the ScaleData function in Seurat. After performing PCA, a number of principle components were selected from an elbow plot and used to generate UMAPs for each dataset. For all datasets, clusters were then determined using the FindClusters function in Seurat. A small cluster of cells labeled as T cells in the Ordovas-Montanes *et al.* dataset appeared to represent eosinophils and was excluded from analysis.

Statistical analysis

Statistical analysis was performed in the R software version 3.5.1. The specific parametric and nonparametric statistical tests are indicated in the figure legends. *P* values <0.05 were considered statistically significant. For differential gene expression analysis, genes with an adjusted $P < 0.001$ and an average log fold change of greater than 0.25 were considered statistically significant.

SUPPLEMENTARY MATERIALS

immunology.sciencemag.org/cgi/content/full/6/62/eabi5586/DC1
Figs. S1 to S13
Table S1
Data files S1 to S8

View/request a protocol for this paper from *Bio-protocol*.

REFERENCES AND NOTES

1. G. T. Furuta, D. A. Katzka, Eosinophilic esophagitis. *N. Engl. J. Med.* **373**, 1640–1648 (2015).
2. B. P. Davis, M. E. Rothenberg, Mechanisms of disease of eosinophilic esophagitis. *Annu. Rev. Pathol. Mech. Dis.* **11**, 365–393 (2016).
3. N. Gonsalves, G.-Y. Yang, B. Doerfler, S. Ritz, A. M. Ditto, I. Hirano, Elimination diet effectively treats eosinophilic esophagitis in adults; food reintroduction identifies causative factors. *Gastroenterology* **142**, 1451–1459.e1 (2012).
4. D. A. Hill, J. M. Spergel, The immunologic mechanisms of eosinophilic esophagitis. *Curr. Allergy Asthma Rep.* **16**, 9 (2016).
5. M. Rochman, N. P. Azouz, M. E. Rothenberg, Epithelial origin of eosinophilic esophagitis. *J. Allergy Clin. Immunol.* **142**, 10–23 (2018).
6. J. D. Sherrill, K. KC, C. Blanchard, E. M. Stucke, K. A. Kemme, M. H. Collins, J. P. Abonia, P. E. Putnam, V. A. Mukkada, A. Kaul, S. A. Kocoshis, J. P. Kushner, A. J. Plassard, R. A. Karns, P. J. Dexheimer, B. J. Aronow, M. E. Rothenberg, Analysis and expansion of the eosinophilic esophagitis transcriptome by RNA sequencing. *Genes Immun.* **15**, 361–369 (2014).
7. L. C. Kottyan, M. E. Rothenberg, Genetics of eosinophilic esophagitis. *Mucosal Immunol.* **10**, 580–588 (2017).
8. A. Mitson-Salazar, Y. Yin, D. L. Wansley, M. Young, H. Bolan, S. Arceo, N. Ho, C. Koh, J. D. Milner, K. D. Stone, S. A. Wank, C. Prussin, Hematopoietic prostaglandin D synthase defines a proeosinophilic pathogenic effector human T_H2 cell subpopulation with enhanced function. *J. Allergy Clin. Immunol.* **137**, 907–918.e9 (2016).
9. T. Wen, B. J. Aronow, Y. Rochman, M. Rochman, K. KC, P. J. Dexheimer, P. Putnam, V. Mukkada, H. Foote, K. Rehn, S. Darko, D. Douek, M. E. Rothenberg, Single-cell RNA sequencing identifies inflammatory tissue T cells in eosinophilic esophagitis. *J. Clin. Invest.* **129**, 2014–2028 (2019).
10. T. M. Gierahn, M. H. Wadsworth II, T. K. Hughes, B. D. Bryson, A. Butler, R. Satija, S. Fortune, J. C. Love, A. K. Shalek, Seq-Well: Portable, low-cost RNA sequencing of single cells at high throughput. *Nat. Methods* **14**, 395–398 (2017).
11. T. K. Hughes, M. H. Wadsworth, T. M. Gierahn, T. Do, D. Weiss, P. R. Andrade, F. Ma, B. J. de Andrade Silva, S. Shao, L. C. Tsoi, J. Ordovas-Montanes, J. E. Gudjonsson, R. L. Modlin, J. C. Love, A. K. Shalek, Second-strand synthesis-based massively parallel scRNA-seq reveals cellular states and molecular features of human inflammatory skin pathologies. *Immunity* **53**, 878–894.e7 (2020).
12. L. McInnes, J. Healy, J. Melville, UMAP: Uniform manifold approximation and projection for dimension reduction, arXiv:1802.03426 [stat.ML] (2018).
13. V. Gruart, M. J. Truong, J. Plumas, M. Zandecki, J. P. Kusnierz, L. Prin, D. Vinatier, A. Capron, M. Capron, Decreased expression of eosinophil peroxidase and major basic protein messenger RNAs during eosinophil maturation. *Blood* **79**, 2592–2597 (1992).
14. J. Bystrom, K. Amin, D. Bishop-Bailey, Analysing the eosinophil cationic protein—A clue to the function of the eosinophil granulocyte. *Respir. Res.* **12**, 10 (2011).
15. S. Kaur, J. M. Rosen, A. A. Kriegermeier, J. B. Wechsler, A. F. Kagalwalla, J. B. Brown, Utility of gastric and duodenal biopsies during follow-up endoscopy in children with eosinophilic esophagitis. *J. Pediatr. Gastroenterol. Nutr.* **65**, 399–403 (2017).
16. S. Aibar, C. B. González-Blas, T. Moerman, V. A. Huynh-Thu, H. Imrichova, G. Hulselmans, F. Rambow, J.-C. Marine, P. Geurts, J. Aerts, J. van den Oord, Z. K. Atak, J. Wouters, S. Aerts, SCENIC: Single-cell regulatory network inference and clustering. *Nat. Methods* **14**, 1083–1086 (2017).
17. C. Schwartz, R. Willebrand, S. Huber, R. A. Rupec, D. Wu, R. Locksley, D. Voehringer, Eosinophil-specific deletion of IκBα in mice reveals a critical role of NF-κB-induced Bcl-x_L for inhibition of apoptosis. *Blood* **125**, 3896–3904 (2015).
18. C. Bouffi, M. Rochman, C. B. Zust, E. M. Stucke, A. Kartashov, P. C. Fulkerson, A. Barski, M. E. Rothenberg, IL-33 markedly activates murine eosinophils by an NF-κB–dependent mechanism differentially dependent upon an IL-4–driven autoinflammatory loop. *J. Immunol.* **191**, 4317–4325 (2013).
19. L. M. Judd, R. G. Heine, T. R. Menheniott, J. Buzzelli, N. O'Brien-Simpson, D. Pavlic, L. O'Connor, K. Al Gazali, O. Hamilton, M. Scurr, A. M. Collison, J. Mattes, K. J. Allen, A. S. Giraud, Elevated IL-33 expression is associated with pediatric eosinophilic esophagitis, and exogenous IL-33 promotes eosinophilic esophagitis development in mice. *Am. J. Physiol. Gastrointest Liver Physiol.* **310**, G13–G25 (2016).
20. D. Hoppenot, K. Malakauskas, S. Lavinskiene, R. Sakalauskas, p-STAT6, PU.1, and NF-κB are involved in allergen-induced late-phase airway inflammation in asthma patients. *BMC Pulm. Med.* **15**, 122 (2015).
21. M. Gutierrez-Arcelus, N. Teslovich, A. R. Mola, R. B. Polidoro, A. Nathan, H. Kim, S. Hannes, K. Slowikowski, G. F. M. Watts, I. Korsunsky, M. B. Brenner, S. Raychaudhuri, P. J. Brennan, Lymphocyte innateness defined by transcriptional states reflects a balance between proliferation and effector functions. *Nat. Commun.* **10**, 687 (2019).
22. W. W. Agace, Tissue-tropic effector T cells: Generation and targeting opportunities. *Nat. Rev. Immunol.* **6**, 682–692 (2006).
23. J. W. Griffith, C. L. Sokol, A. D. Luster, Chemokines and chemokine receptors: Positioning cells for host defense and immunity. *Annu. Rev. Immunol.* **32**, 659–702 (2014).
24. T. Suply, S. Hannedouche, N. Carte, J. Li, B. Grosshans, M. Schaefer, L. Raad, V. Beck, S. Vidal, A. Hiou-Feige, N. Beluch, S. Barbieri, J. Wirsching, N. Lageyre, F. Hillger, C. Debon, J. Dawson, P. Smith, V. Lannoy, M. Detheux, F. Bitsch, R. Falchetto, T. Bouwmeester, J. Porter, B. Baumgarten, K. Mansfield, J. M. Carballido, K. Seuwen, F. Bassilana, A natural ligand for the orphan receptor GPR15 modulates lymphocyte recruitment to epithelia. *Sci. Signal.* **10**, eaal0180 (2017).
25. A. Habtezion, L. P. Nguyen, H. Hadeiba, E. C. Butcher, Leukocyte trafficking to the small intestine and colon. *Gastroenterology* **150**, 340–354 (2016).
26. L. Xiong, J. W. Dean, Z. Fu, K. N. Oliff, J. W. Bostick, J. Ye, Z. E. Chen, M. Mühlbauer, L. Zhou, Ahr-Foxp3-RORγt axis controls gut homing of $CD4^+$ T cells by regulating GPR15. *Sci. Immunol.* **5**, eaaz7277 (2020).
27. C. A. Tibbitt, J. M. Stark, L. Martens, J. Ma, J. E. Mold, K. Deswarte, G. Oliynyk, X. Feng, B. N. Lambrecht, P. De Bleser, S. Nylén, H. Hammad, M. Arsenian Henriksson, Y. Saeys, J. M. Coquet, Single-cell RNA sequencing of the T helper cell response to house dust mites defines a distinct gene expression signature in airway Th2 cells. *Immunity* **51**, 169–184.e5 (2019).
28. H. Kuwata, S. Hara, Role of acyl-CoA synthetase ACSL4 in arachidonic acid metabolism. *Prostaglandins Other Lipid Mediat.* **144**, 106363 (2019).
29. H. Shindou, D. Hishikawa, H. Nakanishi, T. Harayama, S. Ishii, R. Taguchi, T. Shimizu, A single enzyme catalyzes both platelet-activating factor production and membrane biogenesis of inflammatory cells: Cloning and characterization of acetyl-CoA:lyso-PAF acetyltransferase. *J. Biol. Chem.* **282**, 6532–6539 (2007).
30. W. Tang, M. Bunting, G. A. Zimmerman, T. M. McIntyre, S. M. Prescott, Molecular cloning of a novel human diacylglycerol kinase highly selective for arachidonate-containing substrates. *J. Biol. Chem.* **271**, 10237–10241 (1996).
31. C. Bangert, K. Rindler, T. Krausgruber, N. Alkon, F. M. Thaler, H. Kurz, T. Ayub, D. Demirtas, N. Fortelny, V. Vorstandlechner, W. M. Bauer, T. Quint, M. Mildner, C. Jonak, A. Elbe-Bürger, J. Griss, C. Bock, P. M. Brunner, Persistence of mature dendritic cells, T_H2A, and Tc2 cells characterize clinically resolved atopic dermatitis under IL-4Rα blockade. *Sci. Immunol.* **6**, eabe2749 (2021).
32. J. Ordovas-Montanes, D. F. Dwyer, S. K. Nyquist, K. M. Buchheit, M. Vukovic, C. Deb, M. H. Wadsworth, T. K. Hughes, S. W. Kazer, E. Yoshimoto, K. N. Cahill, N. Bhattacharyya, H. R. Katz, B. Berger, T. M. Laidlaw, J. A. Boyce, N. A. Barrett, A. K. Shalek, Allergic inflammatory memory in human respiratory epithelial progenitor cells. *Nature* **560**, 649–654 (2018).
33. A. A. Tu, T. M. Gierahn, B. Monian, D. M. Morgan, N. K. Mehta, B. Ruiter, W. G. Shreffler, A. K. Shalek, J. C. Love, TCR sequencing paired with massively parallel 3′ RNA-seq reveals clonotypic T cell signatures. *Nat. Immunol.* **20**, 1692–1699 (2019).
34. E. Wambre, V. Bajzik, J. H. DeLong, K. O'Brien, Q.-A. Nguyen, C. Speake, V. H. Gersuk, H. A. DeBerg, E. Whalen, C. Ni, M. Farrington, D. Jeong, D. Robinson, P. S. Linsley, B. P. Vickery, W. W. Kwok, A phenotypically and functionally distinct human T_H2 cell subpopulation is associated with allergic disorders. *Sci. Transl. Med.* **9**, eaam9171 (2017).
35. K. de Ruiter, S. P. Jochems, D. L. Tahapary, K. A. Stam, M. König, V. van Unen, S. Laban, T. Höllt, M. Mbow, B. P. F. Lelieveldt, F. Koning, E. Sartono, J. W. A. Smit, T. Supali, M. Yazdanbakhsh, Helminth infections drive heterogeneity in human type 2 and regulatory cells. *Sci. Transl. Med.* **12**, eaaw3703 (2020).
36. H. Huang, C. Wang, F. Rubelt, T. J. Scriba, M. M. Davis, Analyzing the *Mycobacterium tuberculosis* immune response by T-cell receptor clustering with GLIPH2 and genome-wide antigen screening. *Nat. Biotechnol.* **38**, 1194–1202 (2020).
37. P. K. Chattopadhyay, J. Yu, M. Roederer, A live-cell assay to detect antigen-specific $CD4^+$ T cells with diverse cytokine profiles. *Nat. Med.* **11**, 1113–1117 (2005).
38. B. Upadhyaya, Y. Yin, B. J. Hill, D. C. Douek, C. Prussin, Hierarchical IL-5 expression defines a subpopulation of highly differentiated human Th2 cells. *J. Immunol.* **187**, 3111–3120 (2011).
39. A. Mitson-Salazar, C. Prussin, Pathogenic effector Th2 cells in allergic eosinophilic inflammatory disease. *Front. Med.* **4**, 165 (2017).
40. C. Micossé, L. von Meyenn, O. Steck, E. Kipfer, C. Adam, C. Simillion, S. M. Seyed Jafari, P. Olah, N. Yawlkar, D. Simon, L. Borradori, S. Kuchen, D. Yerly, B. Homey, C. Conrad, B. Snijder, M. Schmidt, C. Schlapbach, Human "T_H9" cells are a subpopulation of PPAR-γ^+ T_H2 cells. *Sci. Immunol.* **4**, eaat5943 (2019).
41. S. A. Islam, D. S. Chang, R. A. Colvin, M. H. Byrne, M. L. McCully, B. Moser, S. A. Lira, I. F. Charo, A. D. Luster, Mouse CCL8, a CCR8 agonist, promotes atopic dermatitis by recruiting IL-5^+T_H2 cells. *Nat. Immunol.* **12**, 167–177 (2011).
42. C. M. Burk, E. S. Dellon, P. H. Steele, Y. V. Virkud, M. Kulis, A. W. Burks, B. P. Vickery, Eosinophilic esophagitis during peanut oral immunotherapy with omalizumab. *J. Allergy Clin. Immunol. Pract.* **5**, 498–501 (2017).
43. A. J. Lucendo, Á. Arias, J. M. Tenias, Relation between eosinophilic esophagitis and oral immunotherapy for food allergy: A systematic review with meta-analysis. *Ann. Allergy, Asthma Immunol.* **113**, 624–629 (2014).
44. J. Cafone, P. Capucilli, D. A. Hill, J. M. Spergel, Eosinophilic esophagitis during sublingual and oral allergen immunotherapy. *Curr. Opin. Allergy Clin. Immunol.* **19**, 350–357 (2019).
45. T. A. Doherty, R. Baum, R. O. Newbury, T. Yang, R. Dohil, M. Aquino, A. Doshi, H. H. Walford, R. C. Kurten, D. H. Broide, S. Aceves, Group 2 innate lymphocytes (ILC2) are

enriched in active eosinophilic esophagitis. *J. Allergy Clin. Immunol.* **136**, 792–794.e3 (2015).
46. J. B. Wechsler, S. M. Bolton, K. Amsden, B. K. Wershil, I. Hirano, A. F. Kagalwalla, Eosinophilic esophagitis reference score accurately identifies disease activity and treatment effects in children. *Clin. Gastroenterol. Hepatol.* **16**, 1056–1063 (2018).
47. E. Z. Macosko, A. Basu, R. Satija, J. Nemesh, K. Shekhar, M. Goldman, I. Tirosh, A. R. Bialas, N. Kamitaki, E. M. Martersteck, J. J. Trombetta, D. A. Weitz, J. R. Sanes, A. K. Shalek, A. Regev, S. A. McCarroll, Highly parallel genome-wide expression profiling of individual cells using nanoliter droplets. *Cell* **161**, 1202–1214 (2015).
48. M. D. Young, S. Behjati, SoupX removes ambient RNA contamination from droplet based single cell RNA sequencing data. bioRxiv 303727 [**Preprint**]. 2018. https://doi.org/10.1101/303727.
49. A. Liberzon, A. Subramanian, R. Pinchback, H. Thorvaldsdóttir, P. Tamayo, J. P. Mesirov, A. Bateman, Databases and ontologies Molecular Signatures Database (MSigDB) 3.0. *Bioinformatics* **27**, 1739–1740 (2011).
50. B. Van de Sande, C. Flerin, K. Davie, M. De Waegeneer, G. Hulselmans, S. Aibar, R. Seurinck, W. Saelens, R. Cannoodt, Q. Rouchon, T. Verbeiren, D. De Maeyer, J. Reumers, Y. Saeys, S. Aerts, A scalable SCENIC workflow for single-cell gene regulatory network analysis. *Nat. Protoc.* **15**, 2247–2276 (2020).
51. J. A. Ramilowski, T. Goldberg, J. Harshbarger, E. Kloppmann, M. Lizio, V. P. Satagopam, M. Itoh, H. Kawaji, P. Carninci, B. Rost, A. R. R. Forrest, A draft network of ligand–receptor-mediated multicellular signalling in human. *Nat. Commun.* **6**, 7866 (2015).

Acknowledgments: We thank our patients and their families who gave their time and participation as well as M. Davila and A. Swensen, the clinical coordinators of this study. **Funding:** This work was supported, in part, by the Koch Institute Support (core) NIH grant P30-CA14051 from the National Cancer Institute, as well as the Koch Institute–Dana-Farber/Harvard Cancer Center Bridge Project. This work was also supported by the Food Allergy Science Initiative at the Broad Institute and the NIH (1UL1TR001102). The MGH Department of Pathology Flow and Image Cytometry Research Core, which provided assistance with FACS, obtained funding from the NIH Shared Instrumentation Program (1S10OD012027-01A1, 1S10OD016372-01, 1S10RR020936-01, and 1S10RR023440-01A1). **Author contributions:** W.G.S., J.C.L., D.M.M., and B.R. conceptualized the study. Q.Y. and N.V.-H. recruited and phenotyped patients and obtained the clinical samples. D.M.M., B.R., N.P.S., and B.E.S. conducted experiments. D.M.M., A.A.T., and B.M. performed bioinformatic analyses. D.M.M., B.R., W.G.S., and J.C.L. wrote and edited the manuscript. **Competing interests:** W.G.S., J.C.L., D.M.M., and B.R. are inventors on a pending patent application at Massachusetts General Hospital that covers the results presented here. W.G.S. serves on the SAB of Aimmune Therapeutics, Allergy Therapeutics, and FARE and is a consultant for ALK, Merck, Nestle, Novartis, Regeneron, and Sanofi. J.C.L. is an advisor and cofounder of Honeycomb Biotechnologies. J.C.L.'s interests are reviewed and managed under MIT's policies for potential conflicts of interests. **Data and materials availability:** Whole-transcriptome and TCR sequencing data from esophageal biopsies, duodenal biopsies, and peripheral blood are available on GEO (accession number GSE175930). Source data files for figures and analysis are available at github.com/duncanmorgan/EoE_SciImmunol or Zenodo (10.5281/zenodo.5047633).

Submitted 17 March 2021
Accepted 14 July 2021
Published 13 August 2021
10.1126/sciimmunol.abi5586

Citation: D. M. Morgan, B. Ruiter, N. P. Smith, A. A. Tu, B. Monian, B. E. Stone, N. Virk-Hundal, Q. Yuan, W. G. Shreffler, J. C. Love, Clonally expanded, GPR15-expressing pathogenic effector T_H2 cells are associated with eosinophilic esophagitis. *Sci. Immunol.* **6**, eabi5586 (2021).

Science Immunology

Clonally expanded, GPR15-expressing pathogenic effector T_H2 cells are associated with eosinophilic esophagitis

Duncan M. Morgan, Bert Ruiter, Neal P. Smith, Ang A. Tu, Brinda Monian, Brandon E. Stone, Navneet Virk-Hundal, Qian Yuan, Wayne G. Shreffler and J. Christopher Love

Sci. Immunol. **6**, eabi5586.
DOI: 10.1126/sciimmunol.abi5586

Pathogenic esophageal T_H2 cells

Eosinophilic esophagitis (EoE) is an allergic disease triggered by exposure to food-derived allergens and characterized by chronic type 2 esophageal inflammation. Morgan *et al*. examined tissue-specific immune responses underlying EoE using paired single-cell RNA and TCR sequencing of esophageal, peripheral blood, and duodenal samples collected from patients with EoE. Eosinophils enriched for NF-κB signaling pathways and clonally expanded pathogenic effector T helper 2 (peT $_H$2) cells were elevated in the esophagus of patients with active disease. In peripheral blood, expression of the chemokine receptor GPR15 enriched for milk-reactive T cells and for peT $_H$2 clonotypes also detected in the esophagus. These results suggest that certain food antigen-specific T cells are poised for esophageal homing and provide insight into clonal features of the T_H2 cell response in EoE.